Lab on a Chip

PAPER

View Article Online
View Journal

Cite this: DOI: 10.1039/d0lc00140f

A microfluidic approach for experimentally modelling the intercellular coupling system of a mammalian circadian clock at single-cell level†

Kui Han,‡[a] Long Mei, ‡§[bc] Ruoyu Zhong,[d] Yuhong Pang,[a] Eric Erquan Zhang*[ce] and Yanyi Huang *[af]

Received 10th February 2020,
Accepted 28th February 2020

DOI: 10.1039/d0lc00140f

rsc.li/loc

In mammals, it is believed that the intercellular coupling mechanism between neurons in the suprachiasmatic nucleus (SCN) confers robustness and distinguishes the central clock from peripheral circadian oscillators. Current *in vitro* culturing methods used in Petri dishes to study intercellular coupling by exogenous factors invariably cause perturbations, such as simple media changes. Here, we design a microfluidic device to quantitatively study the intercellular coupling mechanism of circadian clock at the single cell level, and demonstrate that vasoactive intestinal peptide (VIP) induced coupling in clock mutant *Cry1-/-* mouse adult fibroblasts engineered to express the VIP receptor, VPAC2, is sufficient to synchronize and maintain robust circadian oscillations. Our study provides a proof-of-concept platform to reconstitute the intercellular coupling system of the central clock using uncoupled, single fibroblast cells *in vitro*, to mimic SCN slice cultures *ex vivo* and mouse behavior *in vivo* phenotypically. Such a versatile microfluidic platform may greatly facilitate the studies of intercellular regulation networks, and provide new insights into the coupling mechanisms of the circadian clock.

Introduction

In mammals, the circadian rhythm is dominated by the master clock in the suprachiasmatic nucleus (SCN),[1,2] which emerges from cell-autonomous processes.[3,4] Robust, rhythmic expression of clock genes within the SCN is necessary for the generation of circadian rhythms throughout the brain and body. It has been reported that the intact SCN clock, either in explant cultures *ex vivo* or within the mouse brain *in vivo*, shows robust oscillations against genetic perturbations, such as mutations in core clock genes.[5] While the intracellular clock in individual fibroblasts or dispersed, single SCN neurons of certain clock gene mutants rapidly lose their rhythmicity,[5] a coupling mechanism has been proposed to confer robustness and establish intercellular synchrony through neuropeptides in the intact SCN. Thus, it is this intercellular coupling mechanism that distinguishes the master or central pacemaker in the SCN from slave or peripheral oscillators.[2,5–7]

In SCN neurons, as well as most other mammalian cells, the endogenous, intracellular clock mechanism is composed of a transcription–translation feedback loop (TTFL). This core loop generates a ~24 hour oscillation of clock and clock-controlled gene expression, which governs daily rhythms in various biological progresses. In addition to this core loop, SCN-specific neuropeptides, such as vasoactive intestinal peptide (VIP)[7] and arginine vasopressin peptide (AVP),[8] as well as certain general neurotransmitters including gamma-aminobutyric acid (GABA),[9,10] are believed to contribute to the robustness of these clock gene rhythms. VIP has been identified as an important player in SCN coupling and binds to its receptor VPAC2[11] on the cell membrane. This triggers expression of the *Period* (*Per*) and *Cryptochrome* (*Cry*) genes through cAMP responsive elements (CREs). Loss of functions for VIP or VPAC2 lead to desynchronization of the SCN, suggesting the requirement of this signal pathway.[7] It is still unclear, however, whether VIP-mediated signaling is

[a] *Biomedical Pioneering Innovation Center (BIOPIC), Beijing Advanced Innovation Center for Genomics (ICG), College of Engineering, College of Chemistry, and Peking-Tsinghua Center for Life Sciences, Peking University, Beijing 100871, China. E-mail: yanyi@pku.edu.cn*
[b] *PTN Joint Graduate Program, School of Life Sciences, Peking University, Beijing 100871, China*
[c] *National Institute of Biological Sciences, Beijing 102206, China. E-mail: zhangerquan@nibs.ac.cn*
[d] *Integrated Science Program, Yuanpei College, Peking University, Beijing 100871, China*
[e] *Tsinghua Institute of Multidisciplinary Biomedical Research, Tsinghua University, Beijing 102206, China*
[f] *Chinese Institute for Brain Research, Beijing 102206, China*
† Electronic supplementary information (ESI) available. See DOI: 10.1039/d0lc00140f
‡ These authors contributed equally to this work.
§ Current address: Neuroscience Institute, Department of Psychiatry, School of Medicine, New York University, New York 10016, USA.

sufficient to generate robust coupling among SCN neurons.[5] Importantly, circadian rhythms can be rescued in *Cry1-/-* SCN slices and dispersed SCN neurons by supplying external VIP, and the degree of synchrony of SCN neurons is also sensitive to the phase and dosage of VIP.[12] Dissociated SCN neurons have been used to study circadian clocks at the single-cell level;[5,7] however, the complexity of neuronal cultures and the fact that only a small percentage of neurons secrete VIP has caused many technical difficulties.

Current methods of culturing SCN and other cells in Petri dish present several challenges. It is typically quite difficult to expose cultures to drugs or other treatments without unwanted side-effects impacting on the circadian clock. For example, a simple media change causes serum shock-like perturbatoin,[13] as well as temperature fluctuations,[14] which disrupt circadian oscillations in cultured SCN and cells. In addition, manually changing media can be time-consuming and labor-intensive. Microfluidic perfusion devices[15] are promising tools to overcome these problems because they can be automated systems that use continuous or periodic perfusion of cell cultures.[16,17] In this study, we developed a new microfluidic system to quantitatively study circadian rhythms at the single cell level. We first engineered mouse adult fibroblast (MAF) cell lines from different clock mutant backgrounds to ectopically express the VIP receptor, VPAC2, for subsequent treatment with VIP to synchronize their molecular clocks. These cell lines provide an ideal system in which to study coupling between circadian clock of single cells through the bioluminescence observation. We then built a microfluidic culture and perfusion system, where the engineered MAF cells could be cultured on a microfluidic chip with a programmable fluidic delivery system to apply specific treatments, such as timed VIP pulses. This device fits on a microscope and possesses four chambers within a single microscopic field of view, enabling multiplex measurements, which can greatly shorten experimental periods, and provide direct comparison of multiple cell lines from different genetic backgrounds. A microscope with an ultra-sensitive CCD camera was used for quantitative bioluminescence imaging. We systematically investigated the circadian clocks of our engineered MAF cells and studied the coupling mechanism between single cells. We believe that our microfluidic platform is a promising approach for rapid, as well as long-term, live imaging of single-cell circadian clocks and the interplay in between, particularly to investigate the instant reactions of cells to external stimulations, and other biological oscillators.

Results and discussion

Establishment of the cell lines and VIP stimulation

It is critical to have a stable cellular system for studying circadian clocks. We constructed different MAF cell lines expressing the VIP receptor VPAC2 with a luciferase-containing reporter, including *Cry1-/-*, *Per2-/-* and *Bmal1-/-* cell lines (Fig. S1†). Using the *Cry1-/-* clock mutant cell lines expressing VPAC2, we initially performed experiments on cell populations by plating cells in 35 mm Petri dishes and monitoring luminescence in a population-level photodetector-based instrument (Lumi-Cycle, Actimetrics, US).[18] At the population level, these cells are arrhythmic,[5] and only become synchronized when treated with VIP (Fig. S1D†). Without VIP, *Cry1-/-* cells ectopically expressing VPAC2 cannot sustain rhythms for more than two circadian cycles. In contrast, daily administration of 60 nM VIP restores circadian oscillations in *Cry1-/-* cells. This result demonstrates that the VIP signaling cascade can be successfully engineered into clock mutant fibroblasts to impact the molecular clock and induce intercellular coupling.

Construction of the microfluidic culture and imaging platform

Cell culture on-chip can be performed with various formats using different materials, specifically designed for handling small volume liquid using small quantity of cells. We chose polydimethylsiloxane (PDMS) as the base material for two major reasons. First, gas permeability of PDMS is excellent for long-term cell culture, especially for circadian studies that typically take multiple days or even weeks. Second, PDMS-based, multi-layer microfluidic devices with flexible monolithic pneumatic valves are feasible to program for applications with various steps. Moreover, cells cultured in micro-chambers are well-separated from the lab environment, eliminating any possible pathogen contamination.

The microfluidic device is transparent and suitable for continuous imaging using a microscope (Fig. 1A and B and S2†). Each device has four symmetric units, each containing a cell culture chamber with size of 600 μm × 600 μm × 60 μm (alternatively, another design with two culture chambers was also used in parallel experiments). Four chambers are placed in close proximity so that they fit into a single field-of-view (FOV, Fig. 1C) using an inverted microscope with a 10× objective (UPlanSApo, NA 0.40, Olympus, Japan). In our design, the cell seeding channels are isolated from the medium flowing channels, preventing the possible channel blockage due to the cell death. Control channels are filled with DI water, connected through Tygon tubing as well, and subjected to compressed air in the back. The pressure was applied through a series of solenoid valves that driven by a computer-controlled electronic I/O breakout circuit board.

Each cell culturing chamber is connected to two inlets: one to supply medium and the other to supply chemical stimuli. The whole chip was placed into an on-stage cell culture system (CU-109, Live Cell Instrument, South Korea) to maintain the temperature at 37 °C and a constant humidity for continuous microscopic imaging. The culture medium was pumped by the air pressure, also controlled by solenoid valves. A custom LabVIEW program operated all the solenoid valves so that each monolithically embedded pneumatic

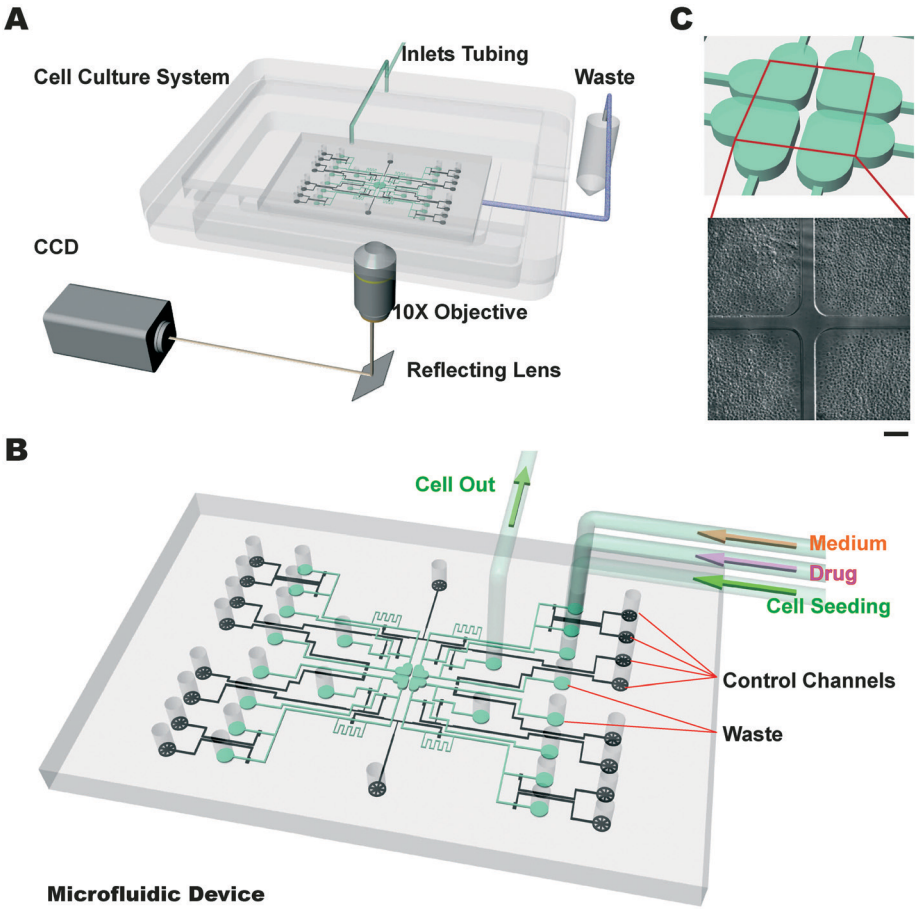

Fig. 1 The experimental scheme and microfluidic design. (A) The setup and the major components in the system, including a cell culture system, which maintains constant temperature and humidity, a 10× objective and a CCD camera. (B) Sketch of a microfluidic device used for studying single cell circadian clock (not scaled). Each device has four identical functional units, and each unit contains a cell culture chamber with size of 600 μm × 600 μm × 60 μm. Four chambers are placed in close proximity fitting into a single field-of-view (FOV) of a 10× objective. Tygon tubing is used to connect the chip with medium supply and external air pressure. Green channels and chambers are used for medium flowing, seeding cells and cell culturing, while black parts are controlling channels and valves. Arrows stand for the medium, drug and cells flowing, respectively. (C) A close-look of the cell culture chambers, and the microphotograph of the camera FOV with cells cultured inside (scale bar: 200 μm).

valves on-chip can be open and closed with designed time series, allowing for the specific flow status of culture medium and chemical stimuli such as VIP introduction. Before seeding cells onto the microfluidic chip, the PDMS surface inside the channels and chambers was treated with a fibronectin solution for two hours.[19] Deionized water was then introduced to rinse the channels, and then the fibronectin-coated surface was air-dried.

To maintain the long-term cell viability, fresh culture medium was pumped into the device continuously at a low velocity to minimize the shear stress applying on cells. The stimulus, VIP, was also pumped into the culture chambers using a separate valve to precisely control the timing and dosage. Waste was collected in separate tubes. Experiments were automated and performed for up to 10 days. Bioluminescence was recorded using a water-cooled ultra-sensitive CCD camera (iKon M-934, Andor, Oxford Instruments, UK) with detector operated at −90 °C. The bioluminescence signal of single cells was extremely weak, hence images were captured with exposure time 30 min, and two images were combined to eliminate noise. Binning was set at 4 × 4 pixels for single cell bioluminescence detection.

Circadian rhythms of cells cultured on a chip

To test the performance of our setup, we firstly measured the collective circadian rhythm of cells cultured on our microfluidic platform through bioluminescence imaging. The *Cry1-/-* MAF cells were used in our study for their coherent circadian oscillations would lose when intercellular coupling is absent, and such coherence could also be restored using periodically introduced VIP as external stimulus. *Cry1-/-* MAF cells were seeded onto a chip cell culture chamber, ensuring confluent packing of cells and the contact between them after adhesion onto the lower surface, which typically took 2 h. Fresh medium was delivered for 10 min every hour at a flow rate *ca.* 1.5 μl min^{-1}, and VIP was perfused for 2 h with a period of 24 h. The first pulsed VIP stimulation was

delivered between the 22nd and 24th hours. The addition of fresh medium to the cells was computer-programmed through the open and close of valves on-chip by controlling the back pressure, and did not interfere with imaging. The average bioluminescent signals can also be quantified by integrating and averaging the imaging data (Fig. 2A and B) in the absence of VIP and in the presence of 60 nM VIP. Beginning of the experiments exhibits high baselines and hence the analysis starts from 12 h. Bioluminescent images taken at different times (Fig. 2C) showed apparent brightness variation with 60 nm VIP pulses in a period of ~24 h. The results observed here in single cells treated with VIP are consistent with the results of our experiments done with cell populations (Fig. S1D†), showing that microfluidic approach is not only able to provide a controllable microenvironment for long-term cell culture, but also offers a much more accurate controllability for culture condition and completely eliminated the risk of contamination compared with Petri-dish-based conventional culture approaches. The VIP introduction is also more accurate and gentler, with less mechanical or temperature perturbations applied to the cell culture. Our data also suggests that, compared with bulk measurement using photomultiplier (PMT) with a specific incubator,[18] the ultra-sensitive CCD-based detector, coupled with microscopes, can be used for highly quantitative assessment using much less cells.

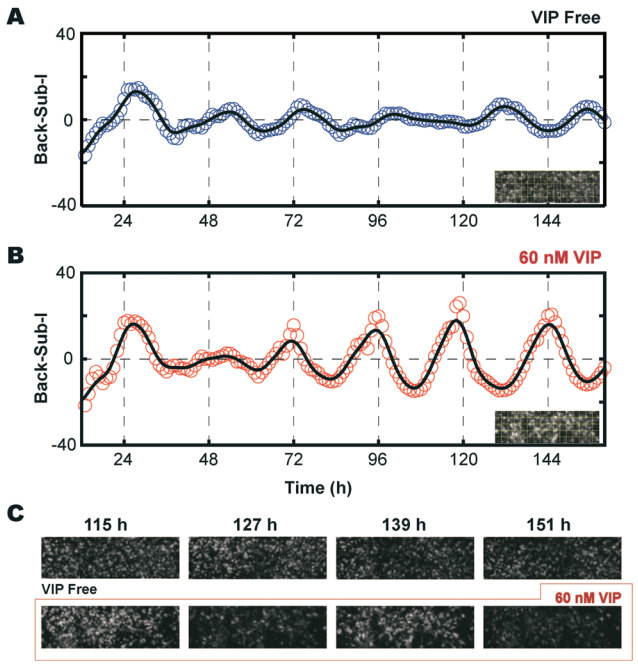

Fig. 2 The average bioluminescent signals for *Cry1-/-* MAF cell population cultured in microfluidic chip (A) in the absence of VIP, and (B) in the presence of 60 nM daily VIP supply. The *Y* axis is the background subtracted intensity (Back-Sub-I). Without VIP supply oscillation damps fast after one circle, while strong circadian oscillation lasts for days with VIP pulses. The results of on-chip culture are consistent with the population experiments. Inserts show the segmentation for each image. (C) Bioluminescent images taken at different times in 36 hours. Images with 60 nm VIP pulses show apparent brightness variation of the bioluminescent signals in a period of ~24 h.

To study the circadian clock in single cells and coupling among cells, we segmented bioluminescent images into small square regions of uniform size, to best capture circadian phases of single cells, depending on the density of the cells, the magnification of the objective, and their migration over the course of the experiment. The cellular level signal process was done through segmentation and processing of microscopic images, which could capture the cellular level circadian signal at high magnification. The cell culture had to be done with population since inter-cellular communication through secretion was necessary for this experiment and for cell viability. However, cells were adherent and each cell occupied ~6 × 6 pixels at a modest mono-layer seeding density. Although the quality of bioluminescence images was not suitable for pixel-level image segmentation to define cell territories, we found that our simple segmentation method suited our experimental requirement, for the study of cells coupling. According to the bioluminescent imaging, the size of segment was determined to fit the seeding density of cells, approximately by the single bright spot's size and trace during the measurement, which was larger than the size of a single cell by counting cells migration. Although the cell migration or locomotion may cause cell number fluctuation within the segments, the overall effect would be the decreased amplitude of the circadian rhythm. This may cause difficulties to identify the weak synchronization between cells, but the population scale inter-cellular coupling would not be obscured by the segmentation method. The advantage of studying inter-cellular coupling of circadian clock using segments is that it avoids the technical challenge of determining each cell's territory with such low intensity bioluminescence signal and blurred image. Hence the intensity of each segment becomes a reasonably good approximation to indicate the circadian rhythm of one single cell. The bioluminescent traces of intensity *versus* time were than analyzed for every segment within the FOV.

All images obtained under different culture conditions were divided into a lattice with segment size of 6 × 6 pixels, and intensity trace of each segment, between the 60th and 156th hours, were recorded and analyzed. The temporal traces of all the segments, as well as the average of them, were plotted (Fig. 3). In the absence of VIP stimulation (Fig. 3A), each segment maintains its circadian oscillation, but the synchronization among them is lost, resulting in arrhythmia. This process can also be illustrated through a heat map of phase (Fig. 3C). In contrast, periodic stimulation with VIP led to intercellular synchrony and robust oscillations of each segment (Fig. 3B and D). It is worth to emphasize that the bioluminescence intensity increase upon VIP stimulation was not caused by serum shock,[13] as in our experiments we control the microfluidic device to exchange culture media continuously. Collectively our results show that the periodic stimulation of VIP not only facilitates

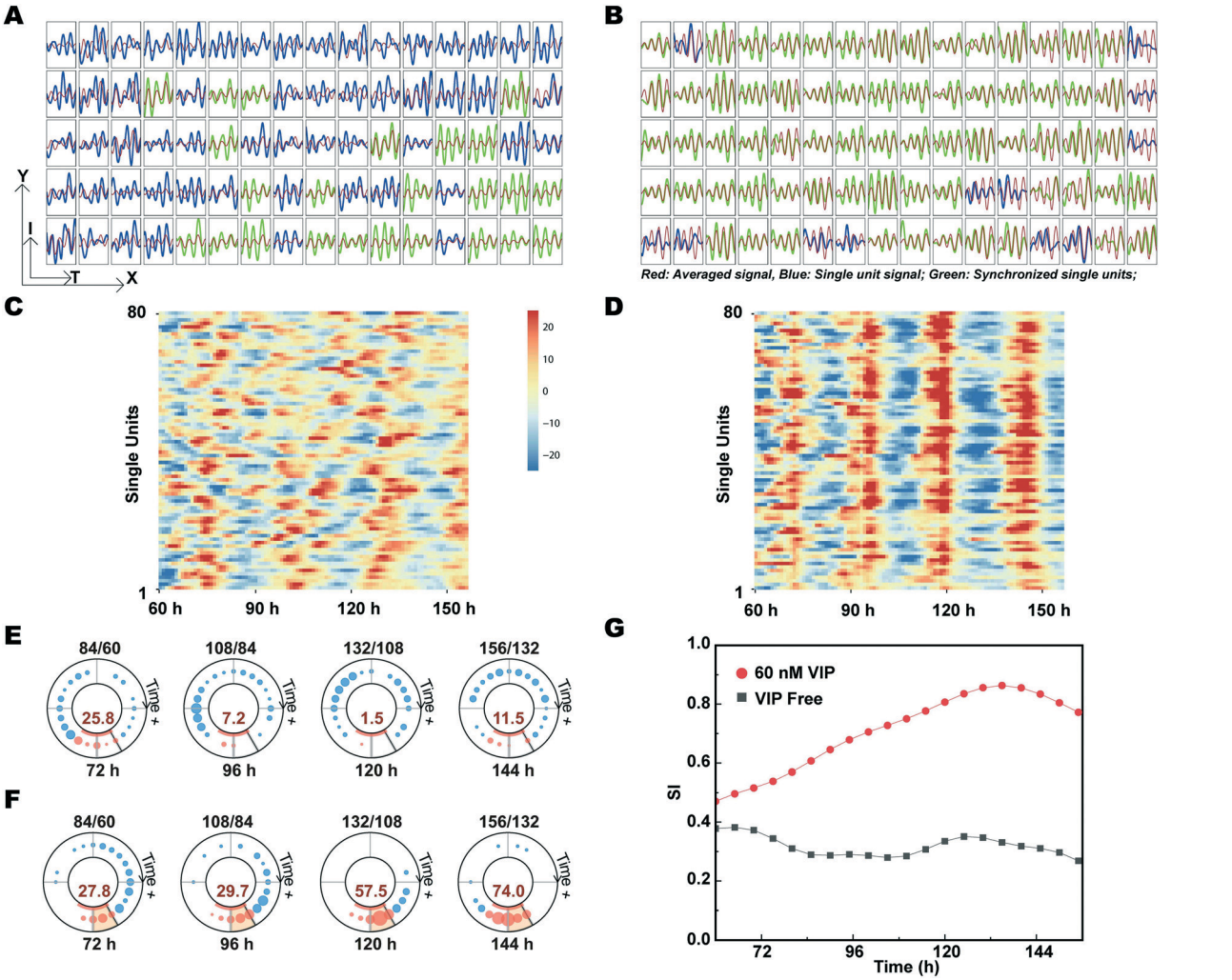

Fig. 3 The temporal traces of all the segments of *Cry1-/-* MAF cells bioluminescent signals (blue) in the absence of VIP (A) and in the presence of 60 nM VIP pulses (B) from 60th h to 156th h. The average signal was plotted in red in each segment, and oscillations of synchronized segments were marked with green. *Y* axis is the background subtracted intensity (Back-Sub-I). Without VIP, each segment maintains its circadian oscillation, but few of them show synchronized behavior. With periodic VIP pulses, most of segments are synchronized, leading to robust and coherent oscillations between segments. (C) and (D) are the signal intensity heatmaps corresponding to (A) and (B), respectively. (E) and (F) peaks distribution of *Cry1-/-* MAF cells circadian oscillations without VIP and with 60 nM VIP, respectively, from 60th h to 156th h. VIP pulse period is marked with orange shadow with time span of 2 h. The percentage of cells whose peaks are synchronized to the VIP pulses is calculated within a time span of 4 h, denoted by a dark red arc on the inner circle. A gradual resetting of phase, with all cells bioluminescence peaking around the time of the VIP induction is observed. The percentage increases from 28% to 74% after the 6th VIP injection. Meanwhile the peaks distribution of cells circadian oscillations without VIP is widespread. (G) Calculated synchronization index (SI) between 60th h and 156th h.

maintaining of circadian oscillations in *Cry1-/-* MAF cells, but also was necessary to reset the oscillation phase and to reestablish synchrony between individual cells.

To better visualize the change in phase and quantitatively assess synchronization among cells within a population, the analyzed the distribution of the peaks of circadian oscillations of all cells (Fig. 3E and F). We treated cells with VIP every 24 hours, and rather than observing a sudden shift in phase, we saw a gradual resetting of phase, with all cells' bioluminescence peaking around the time of the VIP induction (Fig. 3F). The percentage of cells whose peaks were synchronized to the VIP pulses time increased from 28% to 74% after the 6th VIP injection, clearly indicating that the majority of cells have rhythm peaks reset around the VIP stimulation time after a week or so. In contrast, in the absence of VIP, the distribution of the bioluminescence peaks in single cells was widespread (Fig. 3E), and appears loss of synchronization. We use synchronization index (SI)[20,21] to quantitatively represent the phase distribution. The SI characterizes the degree of synchrony between single cells, and is calculated using the equation $SI = |(1/N)\exp(i\varphi_n)|$, where N is the number of cells, and φ_n is the phase difference of the n-th cell with respect to a reference. Here we used the averaged curve of all single cells as reference. SI is calculated with interval of 5 h. The range of SI is from 0 to 1, 0 representing no synchronized behavior between single cells

while 1 representing totally synchronized of all single cells. The higher the SI value, the higher the level of synchronization. Without VIP, the values of SI are very low, while after several VIP pulses, the value of SI increases significantly, indicating the profound effect of VIP on circadian coupling (Fig. 3G). Single cell circadian oscillations were also analyzed in the frequency domain through fast Fourier transform (Fig. S3†). Results show that, with VIP stimulations, over 65% of the single cells analyzed had a circadian period of 23.6 h, which is consistent with the period of VIP stimulation.

The experimental results of VIP-mediated synchronization can also be simulated by an established model[22,23] that contains a set of differential equations describing the reactions in circadian regulatory networks (Fig. S4†). Our simulation on 100 individual segments illustrated the concentration oscillation of key components in the networks and the effect of VIP in the feedback system. We used cytoplasmic concentration of *Per2* mRNA as the indicator of clock phase, and the endogenous VIP secretion was set to 0. We first ran the simulation for 500 h before applying external stimulation of VIP. All the parameters used the same values as the previous model,[22,23] except that the parameter of external VIP pulses was set to zero in the first 500 h, which should be long enough for all cells circadian oscillations to develop separately to form a random oscillations pattern and achieve a homeostatic condition in our simulation. In this way we have simulated the experimental oscillations of the uncoupled MAF cells. Clearly, *Cry1-/-* cells were not synchronized in the absence of VIP (Fig. S5A†), while the intercellular phase lock could be quickly established upon the exposure to VIP, which as applied with a period of 24 h. The circadian synchronization facilitated by rhythmic exposure of VIP can also be quantitatively assessed by SI (Fig. S5B†), which has been significantly elevated. The near perfect agreement between experimental data and simulation results in *Cry1-/-* cells illustrates that our experimental setup provides a useful tool to study intercellular coupling with high precision and accuracy, and to bring new insights into the coupling mechanism between cellular circadian.

This experimental system for microfluidic cell culture and circadian assessment can be applied for studying many other factors that regulated circadian rhythms. For example, in addition to *Cry1*, *Per2* and *Bmal1* are two other core clock genes and also play important roles in circadian clock function of single cells. Homozygous knock-out of either the *Per2* or *Bmal1* gene[5,24] leads to a loss of circadian rhythms in single cells. However, how VIP effects the circadian oscillator in uncoupled *Per2-/-* and *Bmal1-/-* single cells has not yet been studied. To preliminarily test our method on studying the functions of these genes, we hence generated the *Per2-/-* and *Bmal1-/-* MAF cell lines that express VPAC2, and used the same experimental design (Fig. 4).

Interestingly, the *Per2-/-* cells were unlike *Cry1-/-* cells and did not exhibit the regular reconstitution of circadian oscillations when exposed to VIP pulses. The endogenous circadian rhythms of *Per2-/-* cells were rapidly lost in the cell culture, and after introducing VIP, all cells were switched into

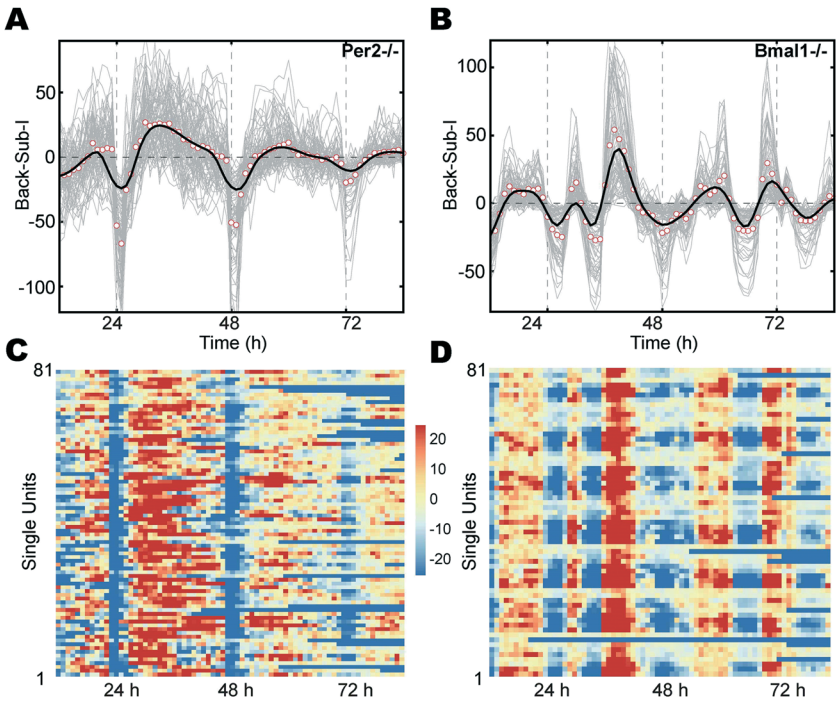

Fig. 4 The circadian responses with *Per2-/-* and *Bmal1-/-* MAF cells. The bioluminescent signals for *Per2-/-* (A) and *Bmal1-/-* (B) MAF cells cultured in microfluidic chip in the presence of VIP, showing different responses compared to *Cry1-/-* MAF cells. Signal from each segment is plotted in grey line, and the average signal of all segments is drawn in red circles, and smoothed as a black line. (C) and (D) are phase heatmap corresponding to (A) and (B) respectively.

a state with low level of bioluminescence. However, this reset action transformed all cells to a level of high bioluminescence with intercellular phase lock after the removal of VIP (Fig. 4A and C), in contrast to monotonic enhancement of bioluminescence by VIP stimulation. Many factors might be involved in this discrepancy, and the unusual response of *Per2-/-* cells to VIP indicates that there are still some unknown factors influencing the intracellular coupling of circadian clocks. Although it has been reported that high concentration of VIP can induce de-synchronization between single cells,[12] however, in our study the low bioluminescent states appear synchronized, as indicated in the single cell traces (Fig. 4A). One possible reason for this might be the timing of VIP treatment is actually more critical than we thought. Previous study also showed that only when VIP is released in phase with the activators of PER expression could synchronize oscillations in the SCN, while anti-phasic treatment with VIP suppressed coherent SCN rhythms.[25] The effect of timed VIP stimulation on different clock mutant cell lines clearly needs further investigations.

As predicted, external timed VIP stimulation appeared to synchronize *Bmal1-/-* MAF cells and restored oscillations in these cells (Fig. 4B and D). However, the period of these single cell oscillations are not consistent with the 24 h period of VIP stimulation. Instead, these oscillations appear stochastic, showing a randomly distributed phase patterns. A previous study[24] showed that dispersed SCN neurons from *Bmal1-/-* mutant mice lost their rhythmicity, while *Bmal1-/-* SCN showed stochastic oscillations with periods that overlap the circadian range. These *in vivo* results are consistent with our observations of VIP-induced intercellular coupling in *Bmal1-/-* single cells *in vitro*.

Conclusions

Intercellular coupling between single clock mutant fibroblast cells was reconstituted *in vitro* by applying microfluidic tools into engineered cell lines with mutations on core clock genes cry1, per2, and bmal1. Microfluidics enabled us to build an automated long-term cell culture system for continuous medium exchange and precisely program-controlled drug exposure. Clock mutant MAF cells were engineered to express the VIP receptor, VPAC2, allowing these cells to sense external VIP. Results from *Cry1-/-* cells stimulated rhythmically with VIP, indicating that VIP signaling synchronizes these cells and rescues circadian oscillations in uncoupled MAF cell lines *in vitro*. These results are consistent with numerical simulations based on the gene regulatory network. Using same microfluidic approach, we also observed the unusual synchronizing effects *Per2-/-* and *Bmal1-/-* cells in response to rhythmic VIP stimulations, suggesting new insights into the intercellular coupling mechanism of the circadian clock. In summary, our microfluidic system offers a proof-of-concept solution to investigate intercellular coupling between clocks of individual cells using exogenous drug exposure and long-term continuous microscopic bioluminescent imaging.

Experimental

Cell lines, medium and drugs

The clock reporter cell lines used in this study were derived from various clock mutant MAF cells and have been reported previously.[5,26–29] Briefly, *Cry1-/-* and *Bmal1-/-* mice were crossed with PER2::LUC knocking mice to generate *Cry1-/-*; PER2::LUC or *Bmal1-/-*; PER2::LUC mice, respectively. Primary fibroblasts were then obtained from mouse tails and used to create immortalized cell lines. To establish *Per2-/-* MAF cells, immortalized *Per2-/-* fibroblasts were infected with a lentiviral-based *mPer2-dLuc* reporter construct (Fig. S1(A)†). All stable cell lines were derived from clones of single cells and have been previously characterized.[5,26–29] To engineer the VIP gene-circuit into our clock mutant MAF cell lines, the *Vipr2* coding sequence fused to a V5 tag was cloned into a lentiviral vector under a cytomegalovirus (CMV) promoter to drive the expression of VPAC2-V5 protein (Fig. S1(B)).†[30] Single cell lines were obtained by sorting transfected cells using flow cytometry, and VPAC2-V5-expressing single cell lines were verified by Western blotting with V5 antibody. Results are shown in Fig. S1(C).† Only cell lines derived from single clones expressing VPAC2-V5 were used in our experiments. Cell lines were cultured in Dulbecco's modified Eagle's medium (DMEM) purchased from Life Technologies (cat#: 12800017). A synthetic version of mature VIP with 28 amino acid residues was obtained from Tocris (cat#: 1911).

Chip fabrication

Soft-lithography technology was employed to fabricate the microfluidic chip. First, AutoCAD was used to draw the pattern of device, which was used to fabricate the mask. Here we employed the push-up mode for chip operation, which possessed three layers with a control layer sandwiched between the flow and glass layers. Second, standard photolithography technology was used to make the mold on a silicon wafer for casting the PDMS. An AZ 50XT (MicroChemicals) was used to fabricate the flow channel with a photoresist thickness of 20 μm, and a SU8-2025 (MicroChemicals) was used to fabricate the cell culture chamber with a thickness of 60 μm and a control layer with a thickness of 20 μm. The flow channel was heated at 190 °C for 17–20 hours to obtain smooth edges. Third, we fabricated the microfluidic device using a RTV 615 A and B, with a mixing ratio of 5 : 1 for the flow layer, 20 : 1 for the control layer and 10 : 1 for the glass layer. The glass layer was spin-coated at a speed of 1800 rpm, obtaining a thin intermediate layer between the control and glass layers. Finally, three layers were bonded together in an 80 °C oven overnight.

Data analysis

Using ImageJ and a custom MATLAB program, we analyzed our bioluminescence data. After images were collected, a pre-treatment was applied by ImageJ to remove outliers.[18] Then, a custom MATLAB program was used to process the imaging

results. The luminescence intensity is too weak for single cell recognition by the images only. Hence, taking cell migration into account, images were segmented using ImageJ with square compartments whose size are around single cells, to mimic 'single-cell' separation, and the average intensity of each compartment was used to represent the circadian rhythm at the single cell level. For temporal analysis, a 24 hour average baseline was subtracted to provide a relative bioluminescence intensity (RBI). All images taken at different times were processed similarly. Finally, based on the RBI from each single cell, a color map was generated for each imaging.

Author contributions

Y. H. and E. E. Z. conceived the idea and designed the study. K. H. designed and fabricated the microfluidic devices. L. M. prepared the mice and cell lines. K. H. and L. M. conducted measurements. K. H. and R. Z. did the data analysis. K. H., L. M., Y. P., E. E. Z, and Y. H. wrote the paper. All authors commented on the manuscript.

Conflicts of interest

There are no conflicts to declare.

Acknowledgements

The authors would like to acknowledge the stimulating discussion with Dr. Samer Hattar at NIMH of NIH, and technical support from Dr. He Chen and Dr. Dapeng Ju. The research was supported by the funds from Ministry of Science and Technology of China (2018YFA0108100 to Y. H.), National Natural Science Foundation of China (21525521 and 21927802 to Y. H., 31971090 to E. E. Z.), Beijing Municipal Government (to E. E. Z.), Beijing Advanced Innovation Center for Genomics (to Y. H.), and Beijing Brain Initiative (Z181100001518004 to Y. H.).

References

1 M. R. Ralph, R. G. Foster, F. C. Davis and M. Menaker, *Science*, 1990, **247**, 975–978.
2 D. K. Welsh, J. S. Takahashi and S. A. Kay, *Annu. Rev. Physiol.*, 2010, **72**, 551–577.
3 S. Yamaguchi, H. Isejima, T. Matsuo, R. Okura, K. Yagita, M. Kobayashi and H. Okamura, *Science*, 2003, **302**, 1408–1412.
4 H. P. Mirsky, A. C. Liu, D. K. Welsh, S. A. Kay and F. J. Doyle, III, *Proc. Natl. Acad. Sci. U. S. A.*, 2009, **106**, 11107–11112.
5 A. C. Liu, D. K. Welsh, C. H. Ko, H. G. Tran, E. E. Zhang, A. A. Priest, E. D. Buhr, O. Singer, K. Meeker, I. M. Verma, F. J. Doyle, III, J. S. Takahashi and S. A. Kay, *Cell*, 2007, **129**, 605–616.
6 R. Silver, J. LeSauter, P. A. Tresco and M. N. Lehman, *Nature*, 1996, **382**, 810–813.
7 S. J. Aton, C. S. Colwell, A. J. Harmar, J. Waschek and E. D. Herzog, *Nat. Neurosci.*, 2005, **8**, 476–483.
8 Y. Yamaguchi, T. Suzuki, Y. Mizoro, H. Kori, K. Okada, Y. Chen, J. Fustin, F. Yamazaki, N. Mizuguchi, J. Zhang, X. Dong, G. Tsujimoto, Y. Okuno, M. Doi and H. Okamura, *Science*, 2013, **342**, 85–90.
9 C. Liu and S. M. Reppert, *Neuron*, 2000, **25**, 123–128.
10 J. A. Evans, T. L. Leise, O. C. Cervantes and A. J. Davidson, *Neuron*, 2013, **80**, 973–983.
11 A. J. Harmar, H. M. Marston, S. Shen, C. Spratt, K. M. West, W. J. Sheward, C. F. Morrison, J. R. Dorin, H. D. Piggins, J. C. Reubi, J. S. Kelly, E. S. Maywood and M. H. Hastings, *Cell*, 2002, **109**, 497–508.
12 S. An, R. Harang, K. Meeker, D. G. Fuentes, C. A. Tsai, C. Mazuski, J. Kim, F. J. Doyle, III, L. R. Petzold and E. D. Herzog, *Proc. Natl. Acad. Sci. U. S. A.*, 2013, **110**, E4355–E4361.
13 A. Balsalobre, F. Damiola and U. Schibler, *Cell*, 1998, **93**, 929–937.
14 E. D. Buhr, S. H. Yoo and J. S. Takahashi, *Science*, 2010, **330**, 379–385.
15 M. A. Unger, H. P. Chou, T. Thorsen, A. Scherer and S. R. Quake, *Science*, 2000, **288**, 113–116.
16 P. J. Hung, P. J. Lee, P. Sabounchi, R. Lin and L. P. Lee, *Biotechnol. Bioeng.*, 2005, **89**, 1–8.
17 S. Giulitti, E. Magrofuoco, L. Prevedello and N. Elvassore, *Lab Chip*, 2013, **13**, 4430–4441.
18 D. K. Welsh, T. Imaizumi and S. A. Kay, *Methods Enzymol.*, 2005, **393**, 269–288.
19 G. K. Toworfe, R. J. Composto, C. S. Adams, I. M. Shapiro and P. Ducheyne, *J. Biomed. Mater. Res., Part A*, 2004, **71**, 449–461.
20 S. H. Strogatz, *Phys. D*, 2000, **143**, 1–20.
21 T. L. To, M. A. Henson, E. D. Herzog and F. J. Doyle, III, *Biophys. J.*, 2007, **92**, 3792–3803.
22 J. K. Kim and D. B. Forger, *Mol. Syst. Biol.*, 2012, **8**, 630.
23 D. DeWoskin, W. Geng, A. R. Stinchcombe and D. B. Forger, *Interface Focus*, 2014, **4**, 20130076.
24 C. H. Ko, Y. R. Yamada, D. K. Welsh, E. D. Buhr, A. C. Liu, E. E. Zhang, M. R. Ralph, S. A. Kay, D. B. Forger and J. S. Takahashi, *PLoS Biol.*, 2010, **8**, e1000513.
25 B. Ananthasubramaniam, E. D. Herzog and H. Herzel, *PLoS Comput. Biol.*, 2014, **10**, e1003565.
26 B. Zheng, U. Albrecht, K. Kaasik, M. Sage, W. Lu, S. Vaishnav, Q. Li, Z. S. Sun, G. Eichele, A. Bradley and C. C. Lee, *Cell*, 2001, **105**, 683–694.
27 G. T. J. van der Horst, M. Muijtjens, K. Kobayashi, R. Takano, S. Kanno, M. Takao, J. de Wit, A. Verkerk, A. P. M. Eker, D. van Leenen, R. Buijs, D. Bootsma, J. H. J. Hoeijmakers and A. Yasui, *Nature*, 1999, **398**, 627–630.
28 M. K. Bunger, L. D. Wilsbacher, S. M. Moran, C. Clendenin, L. A. Radcliffe, J. B. Hogenesch, M. C. Simon, J. S. Takahashi and C. A. Bradfield, *Cell*, 2000, **103**, 1009–1017.
29 S. H. Yoo, S. Yamazaki, P. L. Lowrey, K. Shimomura, C. H. Ko, E. D. Buhr, S. M. Siepka, H. K. Hong, W. J. Oh, O. J. Yoo, M. Menaker and J. S. Takahashi, *Proc. Natl. Acad. Sci. U. S. A.*, 2004, **101**, 5339–5346.
30 G. Tiscornia, O. Singer and I. M. Verma, *Nat. Protoc.*, 2006, **1**, 241–245.

